Published in final edited form as:
Neuron. 2012 January 12; 73(1): 149–158. doi:10.1016/j.neuron.2011.10.030.

Identification of an inhibitory circuit that regulates cerebellar Golgi cell activity

Court Hull and **Wade G. Regehr**[†]
Department of Neurobiology, Harvard Medical School, Boston MA

Summary

Here we provide evidence that revises the inhibitory circuit diagram of the cerebellar cortex. It was previously thought that Golgi cells, interneurons that are the sole source of inhibition onto granule cells, were exclusively coupled via gap junctions. Moreover, Golgi cells were believed to receive GABAergic inhibition from molecular layer interneurons (MLIs). Here we challenge these views by optogenetically activating the cerebellar circuitry to determine the timing and pharmacology of inhibition onto Golgi cells, and by performing paired recordings to directly assess synaptic connectivity. In contrast with current thought, we find that Golgi cells, not MLIs, make inhibitory GABAergic synapses onto other Golgi cells. As a result, MLI feedback does not regulate the Golgi cell network, and Golgi cells are inhibited approximately two milliseconds before Purkinje cells following a mossy fiber input. Hence, Golgi cells and Purkinje cells receive unique sources of inhibition, and can differentially process shared granule cell inputs.

Introduction

The cerebellar cortex plays a crucial role in orchestrating the coordination and timing of body movements (Mauk et al., 2000), and cerebellar deficits or damage typically result in severe ataxia (Grüsser-Cornehls and Bäurle, 2001). At the neural circuit level, timing is often governed by local synaptic inhibition, which is critical for regulating spike timing, population synchrony, and the frequency and amplitude of neural oscillations (Atallah and Scanziani, 2009; Cobb et al., 1995; Mann et al., 2005; Pouille and Scanziani, 2001).

In the cerebellar cortex, inhibition is provided by only a few distinct types of interneurons (Eccles et al., 1966), and the general consensus is that all major pathways of synaptic inhibition have been identified. Of particular importance for local synaptic processing is the cerebellar Golgi cell (D'Angelo, 2008). This interneuron is positioned in the granule cell layer at the input stage of the cerebellar cortex (Fig. 1A). Here, sensory, motor, and higher cognitive information from several brain regions carried by the mossy fibers (MFs) provides strong excitatory drive to both Golgi cells and glutamatergic granule cells (Eccles et al., 1967; Ito, 2006). In turn, Golgi cells generate the sole source of inhibition onto granule cells (Eccles et al., 1964), which are the most numerous cell type in the brain. Golgi cells can also directly inhibit release from MFs by activating presynaptic $GABA_B$ receptors (Mitchell and Silver, 2000). Hence, by regulating the excitability of both granule cells and MFs, Golgi

[†]To whom correspondence should be addressed: Wade Regehr, Goldenson 308, Department of Neurobiology, Harvard Medical School, 220 Longwood Avenue, Boston, MA 02115, Tel: 617-432-0450, Fax: 617-432-1639, wade_regehr@hms.harvard.edu.

cells can gate sensory activation of the cerebellar cortex, and thus have a major impact on cerebellar processing (Galliano et al., 2010).

Golgi cells have indeed been found to play an integral role in cerebellar function. At the behavioral level, acute ablation of Golgi cells results in ataxia (Watanabe et al., 1998). Moreover, Golgi cells are essential for generating behaviorally important temporal patterns of activity in the cerebellum (De Schutter et al., 2000; Isope et al., 2002; Kistler and De Zeeuw, 2003). Electrical connections between Golgi cells mediated by gap junctions on their dendrites allow both synchronous Golgi cell spiking during periods of quiet wakefulness (Dugué et al., 2009), and desynchronized spiking in response to MF activation (Vervaeke et al., 2010).

To understand how Golgi cells make such essential contributions to local cerebellar processing, it is necessary to understand how their activity is regulated by synaptic inhibition. Some of the inhibition onto Golgi cells is generated by rare interneurons called Lugaro cells, which provide a mixed glycinergic/GABAergic input (Dumoulin et al., 2001). However, this input has only been observed *in vitro* in the presence of serotonin (Dieudonné and Dumoulin, 2000), and does not account for the more prominent GABAergic inhibition of Golgi cells. Indirect evidence, both anatomical (Palay and Chan-Palay, 1974) and physiological (Dumoulin et al., 2001), has suggested that molecular layer interneurons (MLIs) inhibit Golgi cells in the same manner as Purkinje cells, and may also be electrically coupled to Golgi cells via gap junctions (Sotelo and Llinás, 1972). Because recent studies have failed to identify inhibitory synaptic connections between Golgi cells (Dugué et al., 2009; Vervaeke et al., 2010), the prevailing view maintains that the Golgi cell network is connected exclusively by gap junctions, and receive GABAergic inhibition from MLIs (Guerts et al., 2003; D'Angelo and De Zeeuw, 2009; De Shutter et al., 2000; Isope et al. 2002; Galliano et al., 2010; Jörntell et al., 2010). This longstanding hypothesis suggests an important functional role for MLIs in providing ongoing feedback inhibition to Golgi cells, and hence in regulating activity throughout the granule cell layer.

Here, we overturn this view by revealing that Golgi cells make inhibitory GABAergic synapses onto each other, and do not receive either inhibitory synapses or electrical connections from MLIs. This indicates that a significant revision to the inhibitory wiring diagram of the cerebellar cortex is needed. Moreover, these newfound connections have functional implications for the timing of inhibition onto Golgi cells, for how these cells are activated, and ultimately for how they regulate MF excitation of the cerebellar cortex.

Results

Golgi cells are known to receive robust GABAergic inhibitory inputs (Dumoulin et al., 2001). Using whole cell voltage-clamp recordings, we find that Golgi cells in cerebellar slices receive a continuous barrage of spontaneous GABAergic inhibitory post-synaptic currents (IPSCs) that are blocked by the $GABA_A$ receptor antagonist gabazine (6.4 ± 1.0 Hz in control and 0.13 ± 0.03 Hz in gabazine, n=6, Fig. 1B). Furthermore, large IPSCs are readily evoked with an extracellular stimulus electrode placed in the granule cell layer near Golgi cell somata (362 ± 51 pA, n=20, Fig. 1C). These IPSCs are predominantly GABAergic, and are abolished by gabazine (5 μM, 3 ± 1% of control, n=19). In one additional cell, a large strychnine sensitive glycinergic component of inhibition was also apparent (Fig. S1A). Hence, all spontaneous inhibition and the vast majority of electrically evoked inhibitory input to Golgi cells is GABAergic. While the spontaneous IPSCs onto Golgi cells suggest that tonically active neurons inhibit Golgi cells, this property cannot be used to identify the source of their inhibition because both MLIs and Golgi cells are spontaneously active.

To explore the source of Golgi cell inhibition, we took advantage of the intact circuitry of a cerebellar brain slice to activate inhibition with a known excitatory input. Hence, an optogenetic approach was used to selectively activate MFs in transgenic mice (Thy1-ChR2/EYFP line 18) that express channelrhodopsin 2 (ChR2) and YFP in a fraction of cerebellar MFs (Fig. 1D, Fig. S2). In these slices, a brief pulse of blue light evoked a compound EPSC onto Golgi cells followed with a latency of 3.1 ± 0.4 ms by a large GABAergic IPSC (control: 207 ± 50 pA, gabazine: 13 ± 6 pA, n = 6, Fig. 1E). This inhibition was polysynaptic, based on the delay between EPSCs and IPSCs, and because it was eliminated by blocking AMPA and NMDA receptors (control: 140 ± 50 pA, NBQX/CPP: 7 ± 7 pA, n = 12, Fig. 1F). In one case, blocking glutamatergic synapses did not abolish inhibition, and this was likely the result of a rare non-glutamatergic (Barmack et al., 1992a; Barmack et al., 1992b; Jaarsma et al., 1997; Kerr and Bishop, 1991) activation of a glycinergic neuron (Fig. S1B)(Dugué et al., 2005; Dumoulin et al., 2001). Hence, inhibition of Golgi cells following activation of the cerebellar MFs is predominantly a robust, polysynaptic input mediated by $GABA_A$ receptors.

As a first step in determining the source of GABAergic input to Golgi cells, we measured the timing of IPSCs evoked by ChR2 stimulation of the MFs. If MLIs inhibit both Golgi cells and Purkinje cells, then the onset of inhibition should occur at the same time in both cell types following MF activation. Surprisingly, in simultaneous recordings from Golgi cells and Purkinje cells (Fig. 2A), the onset of inhibition occurs almost 2 ms earlier in Golgi cells (latency from Golgi cell IPSC to Purkinje cell IPSC = 1.9 ± 0.4 ms, n = 6, p = 0.006; Fig. 2B). This time difference is inconsistent with the same population of interneurons, namely the MLIs, inhibiting Golgi cells and Purkinje cells. Under these experimental conditions, inhibition of Purkinje cells involves three synapses (MF→granule cells→MLIs→Purkinje cells) (Ito, 2006). The shorter latency inhibition of Golgi cells is consistent with a disynaptic inhibition, such as MF→Golgi cell→Golgi cell.

To determine whether the evoked IPSC timing is consistent with Golgi cells inhibiting each other, we compared the timing of inhibition received by Golgi cells and granule cells, which are only inhibited by Golgi cells (Ito, 2006) (Fig. 2C). Simultaneous recordings from Golgi and granule cells revealed that inhibition arrives at approximately the same time onto these two cell types following MF activation (latency from granule cell IPSC to Golgi cell IPSC = 0.3 ± 0.1 ms, p = 0.09; Fig. 2D). These data are consistent with Golgi cells inhibiting both granule cells and other Golgi cells.

We further tested the hypothesis that Golgi cells are inhibited primarily by other Golgi cells by assessing the pharmacological sensitivity of inhibition onto Golgi cells and Purkinje cells. Previous studies have shown that Golgi cells are the only inhibitory cell in the cerebellar cortex to express mGluR2, and that the selective group II mGluR agonist (2*R*,4*R*)-APDC strongly hyperpolarizes Golgi cells to silence their spontaneous spiking (Ohishi and Ogawa-meguro, 1994; Watanabe and Nakanishi, 2003). This suggests that APDC should reduce disynaptic inhibition mediated by Golgi cells by making it more difficult for MF or granule cell inputs to evoke spikes. In contrast, APDC should not affect Purkinje cell inhibition, which is provided by MLIs.

We tested the effect of APDC on polysynaptic inhibition following activation of either granule cell parallel fibers (PFs) or MFs (Fig. 3). In these experiments, all evoked inhibitory synaptic currents were eliminated by application of glutamate receptor antagonists, indicating that they were not a result of direct activation of interneurons. In Thy1-ChR2/EYFP mice, optical activation of MFs evoked IPSCs that were significantly reduced by APDC in Golgi cells, but were unaffected in Purkinje cells (Golgi cells: 58 ± 6% reduction of IPSC amplitude, n = 7, p <0.001 Purkinje cells: 2 ± 3% reduction of IPSC amplitude, n =

8, p = 0.63; Fig. 3A). Similarly, using a stimulus electrode to activate the PFs and recruit inhibition onto Golgi and Purkinje cells, we found that APDC selectively reduced evoked IPSCs onto Golgi cells without significantly affecting IPSCs onto Purkinje cells (Golgi cells: 54 ± 15% reduction of IPSC amplitude, n = 5, p = 0.009; Purkinje cells: 11 ± 6% reduction of IPSC amplitude, n = 5, p = 0.20; Fig. 3B). This selective suppression of Golgi cell inhibition by APDC suggests that Golgi cells are inhibited by other Golgi cells rather than by MLIs.

To directly assess whether Golgi cells are synaptically inhibited by other Golgi cells, we performed paired recordings. Experiments were conducted in an external solution containing 4 mM calcium and 1 μM CGP to facilitate recording synaptic connections, because Golgi cell synapses onto granule cells can have a low release probability and may be tonically suppressed by $GABA_B$ receptors (Mapelli et al., 2009). The experimental configuration is shown in Fig. 4A, and the corresponding characterization of the chemical and electrical synapses is shown in Fig. 4B. These experiments revealed several unitary synaptic connections between Golgi cells (10/50 directions, 20% connected, 1 pair = 2 directions; Fig. 4C). All cell pairs were imaged with 2-photon microscopy, and had a morphology consistent with Golgi cells. The average unitary synaptic connection between Golgi cells was 0.33 ± 0.08 nS (n = 10, Fig. 4C), and 3 pairs were connected with reciprocal chemical synapses. Gabazine blocked these unitary synaptic currents in all cases tested (mean gabazine conductance = −0.003 nS, n = 9, p <0.001, Fig. 4C). The latency between the onset of the spike in the presynaptic cells and the IPSC was 1.3 ± 0.1 ms, and there was considerable variability in the IPSC failure rate (Fig. 4C). In addition, we found that all but one of the synaptically connected pairs were also electrically coupled, which is a hallmark of Golgi cells (Dugué et al., 2009; Vervaeke et al., 2010) (gap junctional conductance = 0.38 ± 0.05 nS, n = 6, Fig. 4C). Interestingly, the only pair connected chemically but not electrically had no dendritic overlap in the molecular layer where gap junctions are thought to connect these cells (Vervaeke et al., 2010) (Fig. S3). Importantly, we have also recorded examples of these synaptic connections in 2 mM external calcium without CGP (Fig. S4). These experiments hence provide direct evidence that Golgi cells form inhibitory GABAergic synapses onto other Golgi cells.

Can MLIs also regulate Golgi cell activity?

While we have shown that Golgi cells inhibit each other, and that the timing and pharmacology of Golgi cell inhibition is not consistent with a strong MLI→Golgi cell synaptic connection, we have not excluded the possibility that MLIs could also provide weak synaptic inhibition to Golgi cells. Because MLIs are electrically coupled to each other by gap junctions, and can fire synchronously as a population, small inputs could have a large impact on Golgi cell network activity (Fig. 5A). Hence, we have used dynamic clamp to determine whether weak but synchronous synaptic inhibition could regulate Golgi cell spiking.

Using dynamic clamp to inject inhibitory post-synaptic conductances (IPSGs) at frequencies typical of MLI spiking (Häusser and Clark, 1997), we tested the role of weak inhibition corresponding to only a few small inputs (0.5–1 nS) on Golgi cell spontaneous spiking. As shown in a representative experiment (Fig. 5B, C), these weak synaptic inputs delivered at 5, 10 and 15 Hz slightly decreased the Golgi cell spontaneous firing rate, but strongly controlled the timing of this spiking. For 5Hz stimulation, the Golgi cell fired out of phase with the inhibitory input. As the stimulus frequency was increased, Golgi cells fired less frequently than the inhibitory inputs, but the firing was still phase locked to the inhibition. Hence, even very small inhibitory inputs can reliably phase lock Golgi cell firing (Fig. 5D).

These experiments suggest that Golgi cells are exquisitely sensitive to synchronous inhibitory input, and that even a weak MLI→Golgi cell synaptic connection would allow the MLI network to entrain firing in the Golgi cell network. Hence, it is essential to determine whether there is any synaptic connection at all between MLIs and Golgi cells.

To test the possibility that MLIs also inhibit Golgi cells, we performed paired recordings between MLIs and Golgi cells (Fig. 6A). In these experiments, we found no synaptic inputs in 124 MLI to Golgi cell pairs (61 pairs in 4 mM external calcium and 1 μM CGP and 63 pairs in 2 mM external calcium and no CGP, Fig. 6B). To ensure that we could record unitary IPSCs from MLIs under our recording conditions, we performed paired recordings between MLIs and Purkinje cells (Fig. 6C). In these experiments, 6 of 10 paired recordings showed IPSCs from MLIs onto Purkinje cells (average conductance = 0.4 ± 0.1 nS, n = 6, Fig. 6D). Thus, our paired recordings suggest that MLIs do not make inhibitory synapses onto Golgi cells.

Because our dynamic clamp studies suggest that even a weak MLI→Golgi cell synapse would allow the MLI network to strongly influence the Golgi cell network, we further tested for the presence of a small MLI→Golgi cell synaptic input using a transgenic mouse line in which MLIs express ChR2 (Fig. 7B, Fig. S5). In these experiments, we used full field, high intensity light to stimulate a maximal number of MLIs while recording simultaneously from both a Golgi cell and a nearby Purkinje cell (Fig 7A). Light pulses evoked large inhibitory synaptic currents in all recorded PCs, which is consistent with the activation of many MLIs (Fig. 7C, D, see methods). These synaptic responses were eliminated by the $GABA_A$-receptor antagonist gabazine. In contrast, even though many MLIs were activated in these experiments, we never observed any synaptic input onto simultaneously recorded Golgi cells (n=6).

Previous studies have also suggested that MLIs and Golgi cells are gap junction-coupled (Sotelo and Llinás, 1972). We therefore tested for such connections, but found no electrical coupling between any MLIs and Golgi cells in 31 paired recordings (mean junctional conductance = −0.01 ± 0.01 nS). These experiments, along with the lack of synaptic connections observed in paired recordings and with ChR2 stimulation, suggest that despite the many MLIs in the molecular layer in close proximity to Golgi cell dendrites, MLIs do not make fast inhibitory synapses or gap junctional connections onto Golgi cells.

Functional Consequences of Golgi cell to Golgi cell Inhibition

These findings change the inhibitory wiring diagram of the cerebellar cortex by establishing that Golgi cells are inhibited by other Golgi cells and not by MLIs (Fig. 8A), but what are the consequences of this circuit revision? MF activation evokes IPSCs that arrive earlier onto Golgi cells than onto Purkinje cells (Fig. 2). To determine the implications for Golgi cell activity, we examined the timing of inhibition relative to excitation in these cells. MF activation should excite Golgi cells directly (MF→Golgi cell), and also indirectly by activating granule cell synapses (MF→granule cell→Golgi cell). Indeed, we find that brief, high intensity optical stimulation of MFs can evoke EPSCs onto Golgi cells that consist of two discrete components (Fig. 8B). Using the CB1 receptor agonist WIN 55,212-2 (WIN), which is known to suppress release from granule cells onto Golgi cells (Beierlein et al., 2007), we found a selective reduction of the second component of the EPSC following ChR2 activation (EPSC1: 2 ± 4 % reduction, p = 0.79, EPSC2: 43 ± 6% reduction, p <0.001, n = 7, Fig. 8B,C). The observed delay between EPSC1 and EPSC2 and the pharmacological sensitivity of EPSC2 establishes that the second component of the EPSC is a result of disynaptically activating granule cell synapses.

We then compared the relative timing of evoked IPSCs and EPSCs. These experiments revealed that disynaptic inhibition from Golgi cells and disynaptic excitation from granule cells arrive simultaneously ($\Delta t = 0.1 \pm 0.3$ ms, $n = 11$, $p = 0.8$, Fig. 8D). This is very different from the timing of excitation and inhibition for Purkinje cells (Fig. 8E). IPSCs evoked by ChR2 activation of the MFs arrived onto Purkinje cells approximately 2 ms after a granule cell-mediated EPSC ($\Delta t = 1.8 \pm 0.3$, $n = 12$, $p < 0.001$), similar to what has been demonstrated previously with electrical stimulation of the parallel fibers (Mittmann et al., 2005). This delay defines a temporal window for summating granule cell inputs to Purkinje cells (Mittmann et al., 2005). For Golgi cells, such a window clearly does not exist, and inhibition is temporally matched with granule cell excitation. Hence, the inhibitory circuit between Golgi cells described here is quite different from the inhibitory circuits regulating Purkinje cells, and does not establish a classic timing window for summation of granule cell excitation.

To determine how the timing of Golgi cell inhibition regulates their excitability following an incoming mossy fiber input to the cerebellar cortex, we again utilized dynamic clamp. In these experiments, we delivered an excitatory post-synaptic conductance (EPSG) comprised of sequential MF and granule cell EPSCs that mimic those recorded during ChR2 activation of the mossy fibers (Fig. 8F). By increasing the size of this excitatory input in a stepwise manner, we determined the threshold for producing an action potential in a recorded Golgi cell. We then delivered a fixed-amplitude IPSG corresponding to a typically-sized Golgi cell IPSC using the timing that we previously measured for Golgi cell inhibition. When inhibition onto Golgi cells was properly timed, it significantly increased the threshold stimulation required for generating action potentials. However, when inhibition arrived just 2 ms later, it had no significant effect on the threshold level of excitation required for spiking the Golgi cells (Fig. 8G). Hence, we find that Golgi cell feed-forward inhibition has a powerful role in regulating the excitability of these cells, which would not be possible if the inhibition came from MLIs.

Discussion

Here we find that, contrary to the accepted view of cerebellar cortical circuitry, Golgi cells receive synaptic inhibition from other Golgi cells and are not inhibited by MLIs. This circuit revision changes our view of how incoming mossy fiber activity is processed by the cerebellar cortex. First, the lack of either chemical or electrical synapses between MLIs and Golgi cells demonstrates that Golgi cell spiking, and hence the excitability of the entire granule cell layer, is not regulated by MLI activity. Second, because Golgi cells receive synaptic inhibition that arrives 2 ms before inhibition onto Purkinje cells, these two cell types can differentially process shared granule cell inputs.

Evidence Supporting a Revised Circuit

Multiple lines of evidence establish that Golgi cells inhibit other Golgi cells. First, following MF activation, Golgi cells and granule cells are inhibited at the same time, whereas Purkinje cells are inhibited two milliseconds later. This timing is consistent with Golgi cells inhibiting one another, because granule cells are inhibited exclusively by Golgi cells, and Purkinje cells are inhibited primarily by MLIs. Second, activating mGluR2 with APDC to hyperpolarize Golgi cells reduces inhibition onto Golgi cells without significantly affecting inhibition onto Purkinje cells. Finally, paired recordings provide direct evidence that Golgi cells make GABAergic synapses onto each other.

Golgi cell inhibition of other Golgi cells appears to be both widespread and prominent. Electrical stimulation produced robust GABAergic inhibition in all Golgi cells tested, suggesting the likelihood that all Golgi cells are inhibited by other Golgi cells. Based on the

size of GABAergic synaptic currents evoked by extracellular stimulation, and the mean unitary conductance of Golgi cell inputs from paired recordings, each Golgi cell is inhibited by at least ten other Golgi cells. At present it is not clear whether the moderate likelihood (20%) of observing synaptic connections between neighboring Golgi cells accurately represents the degree of connectivity *in vivo*, or if technical factors lower the connection rate in our brain slice recordings (see Methods). It is notable that the connection probability between Golgi cells observed here is similar to what has been found for Golgi cell to granule cell inhibitory connections (26%) (Crowley et al., 2009). By comparison, interneuron networks in the neocortex can be either highly synaptically connected (e.g. fast-spiking (FS) basket cells, 20–80% connection probability) (Galarreta and Hestrin, 1999; Galarreta and Hestrin, 2002; Gibson et al., 1999), or exhibit very sparse synaptic connectivity (e.g. low threshold-spiking (LTS) cells, such as Martinotti cells, 0–15% connection probability) (Deans et al., 2001; Gibson et al., 1999). Reports of molecular diversity among Golgi cells (Geurts et al., 2001; Simat et al., 2007) raise the intriguing possibility that only specific subpopulations of Golgi cells are synaptically connected. There is, however, no evidence to date for such an arrangement.

Equally importantly, we have demonstrated that MLIs do not make fast inhibitory synapses or electrical connections onto Golgi cells. No synaptic connections were seen in 124 paired recordings. In addition, ChR2 activation of large numbers of MLIs did not evoke any synaptic response in Golgi cells, suggesting that even weak or sparse synaptic connections from MLIs to Golgi cells do not exist. Given that MLIs provide such strong inhibition to other cell types with dendrites in the molecular layer (Purkinje cells and other MLIs), it is remarkable that Golgi cells are not also inhibited by MLIs. The lack of synaptic connections between MLIs and Golgi cells, despite the close proximity of MLI axons and Golgi cell dendrites, indicates that there must be some molecular mechanism preventing the formation of these synapses.

Functional Implications of Revised Circuitry

We find that even weak inhibition is sufficient to entrain Golgi cells, as long as the inputs are synchronous (Fig. 5). Thus, our finding that Golgi cells and MLIs are not connected by either chemical or electrical synapses is crucial for understanding how activity in the granule cell layer is regulated. Specifically, the network activity of MLIs cannot influence the population of Golgi cells; MLIs are thus only responsible for regulating the excitability of Purkinje cells and other MLIs.

Differences in the sources of inhibition onto Golgi cells and Purkinje cells also have important implications for how these cells process granule cell inputs. Previously, Golgi cells were thought to be similar to Purkinje cells with respect to granule cell excitation and feedforward inhibition from MLIs. As a direct consequence of the Golgi cell to Golgi cell inhibition described here, the timing of inhibition onto Golgi cells and Purkinje cells is quite different. Inhibition onto Purkinje cells is produced in a feedforward manner by granule cell activation of MLIs, and as a result Purkinje cells are inhibited about 1–2 ms after they are excited by the granule cell parallel fibers (Mittmann et al., 2005). Consequently, there is a brief temporal window in which coincident granule cell activity can summate to generate precisely timed Purkinje cell spiking (Mittmann et al., 2005). Though this basic role of feedforward inhibition in controlling spike timing is common in cortical circuits (Gabernet et al., 2005; Mittmann et al., 2005; Pouille and Scanziani, 2001; Wehr and Zador, 2003), the inhibitory circuit regulating granule cell activation of Golgi cells described here is arranged quite differently.

For Golgi cells, MF activation produces disynaptic inhibition from other Golgi cells that arrives simultaneously with disynaptic excitation from the granule cells. With no delay

between the onset of inhibition and granule cell excitation in Golgi cells, inhibition cannot enforce a classical integration time window for granule cell inputs. This suggests that Golgi cell spiking evoked by granule cell activity *in vivo* is unlikely to be precisely timed. Instead, the simultaneous Golgi cell IPSC and granule cell EPSC should generate a net potential that scales with the bulk level of excitation in the circuit, and effectively reduces the amplitude of granule cell excitation. Indeed, our dynamic clamp experiments (Fig. 8 FG) suggest that the timing of Golgi cell inhibition is well-suited to restrict granule cell excitation, and can significantly increase the threshold for stimulation required to spike Golgi cells in response to a combined MF-granule cell input. Hence, rather than enforcing the precise timing of Golgi cell activation with respect to the granule cells, Golgi cell inhibition may act to limit the influence of feedback excitation. This circuit arrangement also may help to explain the observation that when a region of the cerebellar cortex is activated *in vivo*, Golgi cells along a beam of parallel fibers are not activated as synchronously as would be expected given a common excitatory input (Maex et al., 2000).

In contrast with granule cell excitation, Golgi cell inhibition occurs slightly after MF excitation, suggesting that it can establish a temporal window for integrating MF inputs. Previous studies have shown that approximately four MF inputs are needed to trigger a Golgi cell spike (Kanichay and Silver, 2008), and based on the latency of inhibition these inputs would need to arrive within approximately 2 milliseconds. In fact, because Golgi cells and granule cells are inhibited at the same time, inhibition should play a similar role in controlling the integration of MF inputs at these two cell types.

Given the extensive characterization of cerebellar anatomy and physiology, and the importance of Golgi cells to cerebellar function, it is surprising that the inhibitory circuit regulating this central interneuron has been misidentified for so long. With this revised understanding of Golgi cell connectivity, it will be possible to re-examine models of granule cell layer inhibition in response to MF inputs (Albus, 1971; Marr, 1969; Medina et al., 2000), and thus shed new light on how inhibition contributes to information processing at the input stage of the cerebellar cortex.

Experimental Procedures

Slices

Acute slices (250–300 μm thick) were prepared from the cerebellar vermis of postnatal day 17 (P17) - P20 Sprague-Dawley rats, P19-P29 Thy1-ChR2/EYFP line 18 mice (Jackson Labs) (Arenkiel et al., 2007), and Prv-mhChR2-EYFP mice (Jackson Labs) (Zhao et al., 2011). Sagittal slices were used for all experiments, except for those requiring PF electrical stimulation (Fig. 3B) which utilized transverse slices. All experiments requiring ChR2 activation were conducted in slices from Thy1-ChR2/EYFP and Prv-mhChR2-EYFP mice, and all other experiments were conducted in slices from rats, which were of higher quality. Slices were cut in an ice cold solution (Dugué et al., 2005; Forti et al., 2006; Kanichay and Silver, 2008) consisting of (in mM): 130 K-gluconate, 15 KCl, 0.05 EGTA, 20 HEPES, 25 glucose, pH 7.4 with NaOH, and were then stored in a submerged chamber with artificial CSF equilibrated with 95% O_2 and 5% CO_2, consisting of (in mM): 125 NaCl, 26 $NaHCO_3$, 1.25 NaH_2PO_4, 2.5 KCl, 1 $MgCl_2$, 2 $CaCl_2$, and 25 glucose (pH 7.3, osmolarity 310). Slices were initially incubated at 34° C for 25 minutes, and then at room temperature prior to recording. The NMDAR antagonist *R*-CPP (2.5 μM) was added to the cutting and storage solutions to enhance Golgi-cell survival.

Recordings

Visually guided (infrared DIC videomicroscopy and water-immersion 40× objective) whole-cell recordings were obtained with patch pipettes (2–6 MΩ) pulled from borosilicate capillary glass (World Precision Instruments) with a Sutter P-97 horizontal puller. Electrophysiological recordings were performed at 31–33° C. Slices were used within 2 hours of cutting, as synaptic inhibition onto these cells was most readily observed in fresh slices, and Golgi cells tend to die quickly *in vitro*.

IPSCs were recorded at the EPSC reversal potential, and EPSCs were recorded at the IPSC reversal potential, except in paired recordings and Fig. 1B and C where NBQX and CPP were used to block excitation. For experiments recorded at the EPSC reversal potential, the internal pipette solution contained (in mM): 140 Cs-methanesulfonate, 15 HEPES, 0.5 EGTA, 2 TEA-Cl, 2 MgATP, 0.3 NaGTP, 10 phosphocreatine-tris2, 2 QX 314-Cl. pH was adjusted to 7.2 with CsOH. Membrane potentials were not corrected for the liquid junction potential. The IPSC reversal potential for Golgi cells with our cesium internal solution was −64 mV (n=3). The EPSC reversal potential was determined in each experiment by adjusting the membrane potential until no EPSC was evident, and was typically near +15 mV. For paired recordings where current-clamp was necessary, the internal solution contained (in mM): 150 K-gluconate, 3 KCl, 10 HEPES, 0.5 EGTA, 3 MgATP, 0.5 GTP, 5 phosphocreatine-$tris_2$, and 5 phosphocreatine-Na_2. pH was adjusted to 7.2 with NaOH. For some paired recordings, a high Cl^- potassium internal solution was used to increase the driving force for IPSCs (20 of 50 directions in 4 mM external calcium for Golgi to Golgi cell pairs, and 31 of 60 directions in 4 mM external calcium for MLI to Golgi cell pairs). In this internal solution, K-gluconate was replaced with KCl. The IPSC reversal potential for the low Cl^- potassium internal solution was −85 mV (n=3), and +4 mV for the high Cl^- potassium internal (calculated). When converting to conductance values, the direction of the IPSC driving force was defined as a positive conductance. All drugs were purchased from Sigma-Aldrich or Tocris. Paired recordings were only attempted for cells whose somata were within approximately 100 μm.

The modest synaptic connectivity rate between Golgi cells observed here (20%) may result from preferential recording from Golgi cells near the surface of the slice. Because visibility and therefore cell identification is limited deeper within the extremely dense granule cell layer, our recordings were preferentially made from superficial Golgi cells, and this may exacerbate the common problem of severing axonal arborizations in a slice preparation. Indeed, in many instances our fluorescent fills of Golgi cells revealed that all or part of their axon was missing. Other possible factors which could affect the connection probability reported here include a selection bias toward recording from nearby Golgi cells, though the Golgi cell axon can spread more than a millimeter in the sagittal plane (Barmack and Yakhnitsa, 2008).

Data acquisition and analysis

Electrophysiolgical data were acquired using a Multiclamp 700B amplifier (Axon Instruments), digitized at 20 kHz with either a National Instruments USB-6229, a National Instruments PCI-MIO 16E-4 board, or an ITC-18 (Instrutech, Great Neck, NY), and filtered at 2 kHz. Acquisition was controlled both with custom software written in either Matlab (generously provided by Bernardo Sabatini, HMS, Boston, MA), or IgorPro (generously provided by Matthew Xu-Friedman, SUNY Buffalo). Series resistance was monitored in voltage-clamp recordings with a 5 mV hyperpolarizing pulse, and only recordings that remained stable over the period of data collection were used. Glass monopolar electrodes (1–2 MΩ) filled with ACSF in conjunction with a stimulus isolation unit (WPI, A360) were used for extracellular stimulation. EPSC and IPSC latencies were determined by their 5%

rise time, except in Fig. 6, where the peak of the second derivative was used (negative peaks for EPSCs, positive peak for IPSCs). Data are reported as mean ± SEM, and statistical analysis was carried out using the Student's t-test (2-tailed). For all experiments involving APDC and WIN, the % IPSC reduction is measured relative to the average of control and recovery (or antagonist) conditions.

ChR2 stimulation

Slices from Thy1-ChR2/EYFP and Prv-mhChR2-EYFP mice were stored in the dark. A 473 nm blue laser was used to stimulate ChR2 (Optoengine LLC). In the Thy1-ChR2 mice, excitation and inhibition were evoked using full field illumination with either a low intensity (<1 mW under the objective) stimulus for 1–5 ms, or a high intensity stimulus (1–10 mW under the objective) for 0.2 ms. While both regimes were capable of producing a compound MF-granule cell response in Thy1-ChR2 mice, the shorter, high intensity stimulation more effectively separated these components, presumably by generating only brief activity in the MFs. MFs were stimulated at 0.1 Hz. Evoked responses typically ran down with time (as in Figs. 3A and 6C) at the rate of approximately 7% in 10 minutes. In the Prv-mhChR2-EYFP experiments (Fig. 7), MLIs were also stimulated at 0.1 Hz using full field illumination. Based on the mean unitary conductance of MLI→PC synapses (0.4 nS), the mean inhibitory conductance evoked onto PCs in these experiments (12.6 nS), and the 60% connectivity between MLIs and PCs (Fig. 6), we estimate that an average of ~50 MLIs were activated by ChR2 in each paired recording [average = (12.6 nS / 0.4 nS) / 0.6].

Dynamic Clamp

Dynamic clamp recordings were made using the built in dynamic clamp mode of the ITC-18. The AMPAR conductance simulating a combined MF and granule cell EPSC (Fig. 8) was constructed by adding a recorded MF EPSC with a recorded granule cell EPSC from electrical simulation to mimic the EPSCs evoked by ChR2 stimulation of the MFs. The IPSG waveform was taken from a recorded Golgi cell IPSC in response to electrical stimulation (Fig. 1), and was used for both spike-entrainment experiments (Fig. 5) and timing experiments (Fig. 8). AMPAR conductances reversed at 0 mV, while inhibitory conductances reversed at −75 mV. Dynamic clamp recordings were performed in the presence of NBQX (5 μM), CPP (2.5 μM), gabazine (5 μM), and CGP (1 μM). Cells were allowed to rest at their normal potential and spike spontaneously without any injected current. For timing experiments, injected conductances were spike triggered, and timed to occur 100 ms after a spontaneous spike when the afterhyperpolarization (AHP) was completed.

2-photon imaging

Neurons were filled with either 50 μM Alexa 594 hydrazide or 75 μM Alexa 488 hydrazide for 2-photon imaging and morphological characterization. Cells were imaged using a custom 2-photon laser scanning microscope using 800 nm illumination. Images were processed in either ImageJ or Photoshop by adjusting the contrast, brightness, and image noise. For cells where multiple stacks were taken to encompass the entirety of two filled cells, images were aligned by eye.

Supplementary Material

Refer to Web version on PubMed Central for supplementary material.

Acknowledgments

Work was supported by NIH grant R37 NS032405 to WGR.

References

De Schutter E, Vos B, Maex R. The function of cerebellar Golgi cells revisited. Prog brain res. 2000; 124:81–93. [PubMed: 10943118]

Albus JS. A theory of cerebellar function. Math Biosci. 1971; 10:25–61.

Arenkiel BR, Peca J, Davison IG, Feliciano C, Deisseroth K, Augustine GJ, Ehlers MD, Feng G. In vivo light-induced activation of neural circuitry in transgenic mice expressing channelrhodopsin-2. Neuron. 2007; 54:205–218. [PubMed: 17442243]

Atallah BV, Scanziani M. Instantaneous modulation of gamma oscillation frequency by balancing excitation with inhibition. Neuron. 2009; 62:566–577. [PubMed: 19477157]

Barmack NH, Baughman RW, Eckenstein FP. Cholinergic Innervation of the Cerebellum of Rat, Rabbit, Cat, and Monkey as Activity and Immunohistochemistry. J Comp Neurol. 1992a; 317:233–249. [PubMed: 1577998]

Barmack NH, Baughman RW, Eckenstein FP, Shojaku H. Secondary vestibular cholinergic projection to the cerebellum of rabbit and rat as revealed by choline acetyltransferase immunohistochemistry, retrograde and orthograde tracers. J Comp Neurol. 1992b; 317:250–270. [PubMed: 1577999]

Barmack NH, Yakhnitsa V. Functions of interneurons in mouse cerebellum. J Neurosci. 2008; 28:1140–1152. [PubMed: 18234892]

Beierlein M, Fioravante D, Regehr WG. Differential expression of posttetanic potentiation and retrograde signaling mediate target-dependent short-term synaptic plasticity. Neuron. 2007; 54:949–959. [PubMed: 17582334]

Cobb SR, Buhl EH, Halasy K, Paulson O, Somogyi P. Synchronization of neuronal activity in hippocampus by individual GABAergic interneurons. Nature. 1995; 378:75–78. [PubMed: 7477292]

Crowley JJ, Fioravante D, Regehr WG. Dynamics of fast and slow inhibition from cerebellar golgi cells allow flexible control of synaptic integration. Neuron. 2009; 63:843–853. [PubMed: 19778512]

D'Angelo E. The critical role of Golgi cells in regulating spatio-temporal integration and plasticity at the cerebellum input stage. Front neurosci. 2008; 2:35–46. [PubMed: 18982105]

D'Angelo E, De Zeeuw CI. Timing and plasticity in the cerebellum: focus on the granular layer. Trends Neurosci. 2009; 32:30–40. [PubMed: 18977038]

De Schutter E, Vos B, Maex R. The function of cerebellar Golgi cells revisited. Prog. Brain Res. 2000; 124:81–93. [PubMed: 10943118]

Deans MR, Gibson JR, Sellitto C, Connors BW, Paul DL. Synchronous activity of inhibitory networks in neocortex requires electrical synapses containing connexin36. Neuron. 2001; 31:477–485. [PubMed: 11516403]

Dieudonné S, Dumoulin A. Serotonin-driven long-range inhibitory connections in the cerebellar cortex. J Neurosci. 2000; 20:1837–1848. [PubMed: 10684885]

Dugué GP, Brunel N, Hakim V, Schwartz E, Chat M, Lévesque M, Courtemanche R, Léna C, Dieudonné S. Electrical coupling mediates tunable low-frequency oscillations and resonance in the cerebellar Golgi cell network. Neuron. 2009; 61:126–139. [PubMed: 19146818]

Dugué GP, Dumoulin A, Triller A, Dieudonné S. Target-dependent use of co-released inhibitory transmitters at central synapses. J Neurosci. 2005; 25:6490–6498. [PubMed: 16014710]

Dumoulin A, Triller A, Dieudonné S. IPSC kinetics at identified GABAergic and mixed GABAergic and glycinergic synapses onto cerebellar Golgi cells. J Neurosci. 2001; 21:6045–6057. [PubMed: 11487628]

Eccles, J.; Ito, M.; Szentágothai, J. The Cerebellum as a Neuronal Machine. Berlin: Springer; 1967.

Eccles J, Llinas R, Sasaki K. Golgi cell inhibition in the cerebellar cortex. Nature. 1964; 204:1265–1266. [PubMed: 14254404]

Eccles J, Sasaki K, Llinás R. The inhibitory interneurones within the cerebellar cortex. Exp Brain Res. 1966; 1:1–16. [PubMed: 5910941]

Forti L, Cesana E, Mapelli J, D'Angelo E. Ionic mechanisms of autorhythmic firing in rat cerebellar Golgi cells. J Physiol. 2006; 574:711–729. [PubMed: 16690702]

Gabernet L, Jadhav SP, Feldman DE, Carandini M, Scanziani M. Somatosensory integration controlled by dynamic thalamocortical feed-forward inhibition. Neuron. 2005; 48:315–327. [PubMed: 16242411]

Galarreta M, Hestrin S. A network of fast-spiking cells in the neocortex connected by electrical synapses. Nature. 1999; 402:72–75. [PubMed: 10573418]

Galarreta M, Hestrin S. Electrical synapses between GABA-releasing interneurons. Nat Rev Neurosci. 2001; 2:425–433. [PubMed: 11389476]

Galarreta M, Hestrin S. Electrical and chemical synapses among parvalbumin fast-spiking GABAergic interneurons in adult mouse neocortex. Proc Natl Acad Sci USA. 2002; 99:12438–12443. [PubMed: 12213962]

Galliano E, Mazzarello P, D'Angelo E. Discovery and Rediscoveries of Golgi Cells. J Physiol. 2010; 588:3639–3655. [PubMed: 20581044]

Geurts FJ, Timmermans J, Shigemoto R, De Schutter E. Morphological and neurochemical differentiation of large granular layer interneurons in the adult rat cerebellum. Neuroscience. 2001; 104:499–512. [PubMed: 11377850]

Geurts FJ, De Schutter E, Dieudonné S. Unraveling the cerebellar cortex: cytology and cellular physiology of large-sized interneurons in the granular layer. Cerebellum. 2003; 2(4):290–299. [PubMed: 14964688]

Gibson JR, Beierlein M, Connors BW. Two networks of electrically coupled inhibitory neurons in neocortex. Nature. 1999; 402:75–79. [PubMed: 10573419]

Grüsser-Cornehls U, Bäurle J. Mutant mice as a model for cerebellar ataxia. Prog in Neurobiol. 2001; 63:489–540.

Häusser M, Clark BA. Tonic synaptic inhibition modulates neuronal output pattern and spatiotemporal synaptic integration. Neuron. 1997; 19:665–678. [PubMed: 9331356]

Hestrin S, Galarreta M. Electrical synapses define networks of neocortical GABAergic neurons. Trends Neurosci. 2005; 28:304–309. [PubMed: 15927686]

Isope P, Dieudonné S, Barbour B. Temporal organization of Activity in the Cerebellar cortex: A Manifesto for Synchrony. Ann N Y Acad Sci. 2002; 978:164–174. [PubMed: 12582050]

Ito M. Cerebellar circuitry as a neuronal machine. Prog Neurobiol. 2006; 78:272–303. [PubMed: 16759785]

Jaarsma D, Ruigrok TJ, Caffé R, Cozzari C, Levey AL, Mugnaini E, Voogd J. Cholinergic innervation and receptors in the cerebellum. Prog Brain Res. 1997; 114:67–96. [PubMed: 9193139]

Jörntell H, Bengtsson F, Schonewille M, De Zeeuw CI. Cerebellar molecular layer interneurons - computational properties and roles in learning. Trends Neurosci. 2010; 33(11):524–532. [PubMed: 20869126]

Kanichay RT, Silver RA. Synaptic and cellular properties of the feedforward inhibitory circuit within the input layer of the cerebellar cortex. J Neurosci. 2008; 28:8955–8967. [PubMed: 18768689]

Kerr CW, Bishop GA. Topographical organization in the origin of serotoninergic projections to different regions of the cat cerebellar cortex. J Comp Neurol. 1991; 304:502–515. [PubMed: 2022761]

Kistler WM, De Zeeuw CI. Time windows and reverberating loops: a reverse-engineering approach to cerebellar function. Cerebellum. 2003; 2:44–54. [PubMed: 12882234]

Maex R, Vos BP, De Schutter E. Weak common parallel fiber synapses explain the loose synchrony observed between rat cerebellar golgi cells. J Physiol. 2000; 523(Pt 1):175–192. [PubMed: 10673554]

Mann EO, Suckling JM, Hajos N, Greenfield SA, Paulsen O. Perisomatic feedback inhibition underlies cholinergically induced fast network oscillations in the rat hippocampus in vitro. Neuron. 2005; 45:105–117. [PubMed: 15629706]

Mapelli L, Rossi P, Nieus T, D'Angelo E. Tonic activation of GABAB receptors reduces release probability at inhibitory connections in the cerebellar glomerulus. J Neurophys. 2009; 101:3089–3099.

Marr D. A theory of cerebellar cortex. J Physiol. 1969; 202:437–470. [PubMed: 5784296]

Mauk MD, Medina JF, Nores WL, Ohyama T. Cerebellar function: coordination, learning or timing? Curr Biol. 2000; 10:R522–R525. [PubMed: 10898992]

Medina JF, Garcia KS, Nores WL, Taylor NM, Mauk MD. Timing mechanisms in the cerebellum: testing predictions of a large-scale computer simulation. J Neurosci. 2000; 20:5516–5525. [PubMed: 10884335]

Mitchell SJ, Silver RA. GABA spillover from single inhibitory axons suppresses low-frequency excitatory transmission at the cerebellar glomerulus. J Neurosci. 2000; 20:8651–8658. [PubMed: 11102470]

Mittmann W, Koch U, Häusser M. Feed-forward inhibition shapes the spike output of cerebellar Purkinje cells. J Physiol. 2005; 563:369–378. [PubMed: 15613376]

Ohishi H, Ogawa-meguro R. Immunohistochemical Localization of Metabotropic Glutamate Receptors, mGluR2 and mGluR3, in Rat Cerebellar Cortex. Cell. 1994; 13:55–66.

Palay, S.; Chan-Palay, V. Cerebellar cortex. New York: Springer; 1974.

Pouille F, Scanziani M. Enforcement of temporal fidelity in pyramidal cells by somatic feed-forward inhibition. Science. 2001; 293:1159–1163. [PubMed: 11498596]

Simat M, Parpan F, Fritschy J-M. Heterogeneity of Glycinergic and Gabaergic Interneurons in the Granule Cell Layer of Mouse Cerebellum. J Comp Neurol. 2007; 500:71–83. [PubMed: 17099896]

Sotelo C, Llinás R. Specialized membrane junctions between neurons in the vertebrate cerebellar cortex. J Cell Biol. 1972; 53:271–289. [PubMed: 4537207]

Vervaeke K, Lőrincz A, Gleeson P, Farinella M, Nusser Z, Silver RA. Rapid Desynchronization of an Electrically Coupled Interneuron Network with Sparse Excitatory Synaptic Input. Neuron. 2010; 67:435–451. [PubMed: 20696381]

Watanabe D, Inokawa H, Hashimoto K, Suzuki N, Kano M, Shigemoto R, Hirano T, Toyama K, Kaneko S, Yokoi M, et al. Ablation of cerebellar Golgi cells disrupts synaptic integration involving GABA inhibition and NMDA receptor activation in motor coordination. Cell. 1998; 95:17–27. [PubMed: 9778244]

Watanabe D, Nakanishi S. mGluR2 postsynaptically senses granule cell inputs at Golgi cell synapses. Neuron. 2003; 39:821–829. [PubMed: 12948448]

Wehr M, Zador AM. Balanced inhibition underlies tuning and sharpens spike timing in auditory cortex. Nature. 2003; 426:442–446. [PubMed: 14647382]

Zhao S, Ting J, Atallah H, Qiu L, Tan J, Gloss B, Augustine G, Deisseroth K, Luo M, Graybiel A, Feng G. Cell type–specific channelrhodopsin-2 transgenic mice for optogenetic dissection of neural circuitry function. Nature Methods. 2011; 8:745–755. [PubMed: 21985008]

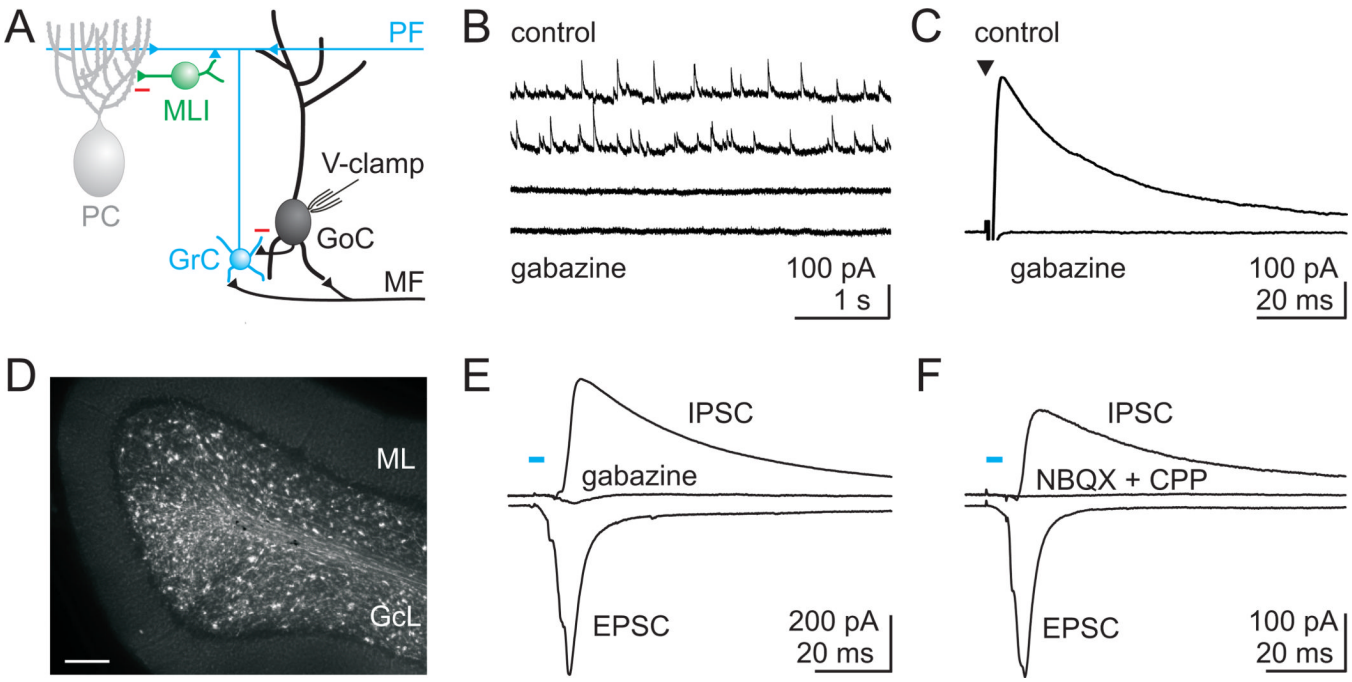

Figure 1. GABAergic inhibitory inputs to Golgi cells

A. Schematic showing the major cell types in the cerebellar cortex with their known synaptic contacts. Abbreviations: PC, Purkinje cell; PF, parallel fiber; MLI, molecular layer interneuron; GrC, granule cell; GoC, Golgi cell; MF, mossy fiber; V-clamp, voltage-clamp. Inhibitory synapses: red minus, and all other synapses (triangles) are glutamatergic. **B.** Spontaneous inhibitory postsynaptic currents (sIPSCs) recorded from Golgi cells at a holding potential of +10 mV in the presence of NBQX (5 μM) and CPP (2.5 μM) to block glutamatergic inputs. All events were blocked by the $GABA_AR$ antagonist gabazine (5 μM). **C.** Average IPSC evoked with a stimulus electrode placed in the granule cell layer near the recorded Golgi cell. Evoked IPSCs were also blocked by gabazine. **D.** Fluorescence image of a cerebellar slice from the vermis of a Thy1 ChR2-YFP mouse that expresses channelrhodopsin 2 (ChR2) and YFP in a subset of MFs. GcL = granule cell layer, ML = molecular layer, Scale bar = 100 μm. **E.** Optical stimulation of ChR2 expressing MFs (473 nm light for 5 ms) evoked EPSCs (recorded at the reversal potential for IPSCs, see methods), and IPSCs (recorded at the EPSC reversal potential). IPSCs evoked by ChR2 activation were blocked by gabazine. **F.** In another experiment, ChR2-evoked IPSCs were also abolished by blocking glutamatergic transmission (NBQX and CPP), indicating that they were disynaptic.

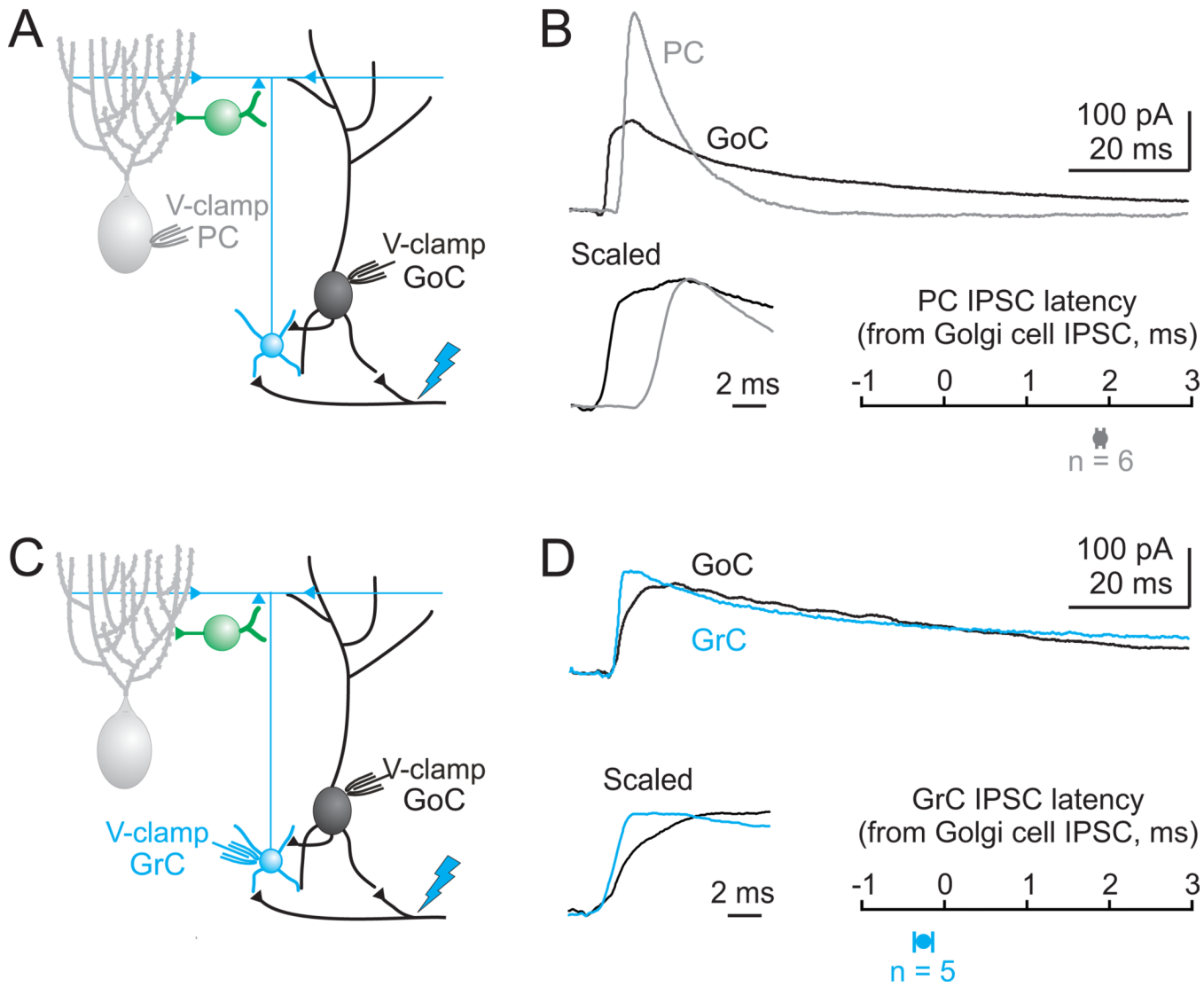

Figure 2. Timing of MF-evoked inhibition onto Golgi cells, Purkinje cells and granule cells

A. Schematic illustrating the recording configuration for B. Blue bolt represents ChR2 activation with 473 nm light. **B.** *top*, Simultaneous recordings from a Purkinje cell (gray) and a Golgi cell (black) at the EPSC reversal potential demonstrate IPSCs onto both cells following ChR2 activation. *bottom, left*. Scaled IPSCs on an expanded timescale show that the Golgi cell IPSC arrives earlier than the Purkinje cell IPSC. *bottom, right*. On average, Golgi cell IPSCs arrived nearly 2 ms earlier than IPSCs onto simultaneously recorded Purkinje cells (n=6). **C.** Schematic of the recording configuration for D. **D.** *top*, Simultaneous recordings of IPSCs evoked by ChR2 activation for a granule cell (blue) and a Golgi cell (black). *bottom, left*. Scaled IPSCs on an expanded timescale show that the Golgi cell IPSC and granule cell IPSC arrive simultaneously. *bottom, right*. On average, for simultaneously recorded Golgi cells and granule cells, IPSCs arrived synchronously (n=5).

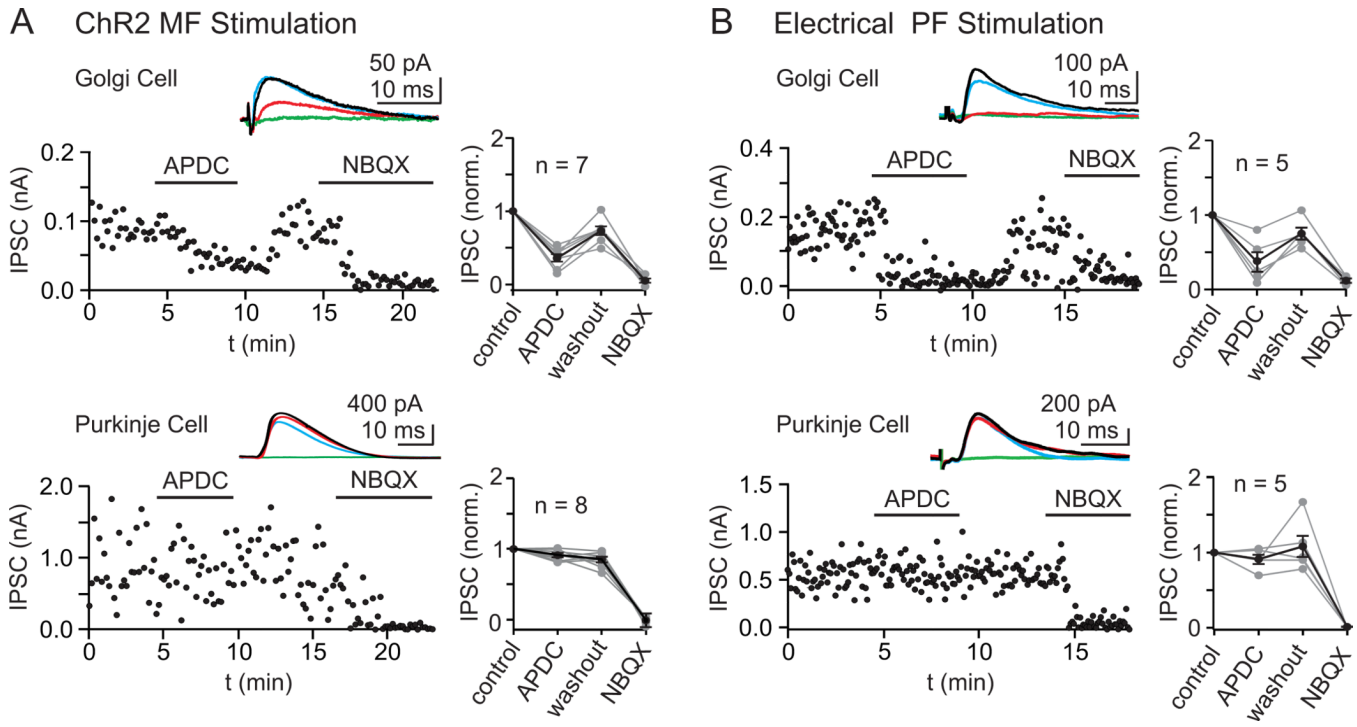

Figure 3. Differential pharmacology IPSCs onto Golgi and Purkinje cells evoked by either MF or PF activation

Following stimulation of either MFs with light (in Thy1 ChR2-YFP mice) (**A**) or PFs with an extracellular stimulus electrode (**B**), the resulting disynaptic IPSCs were recorded at Golgi cells and Purkinje cells, and the pharmacological sensitivity to the selective Group II mGluR agonist APDC (2 μM) was measured. As shown in representative experiments for each condition (**A, B**, *left*) and in the summaries (**A, B**, *right*), Golgi cell IPSCs were strongly attenuated by APDC, but Purkinje cell IPSCs were unaffected. IPSCs in both cells were abolished by blocking glutamatergic transmission (5 μM NBQX and 2.5 μM CPP), indicating that they were disynaptic. Insets show the averaged IPSCs in control (black), APDC (red), washout (blue), and NBQX (green).

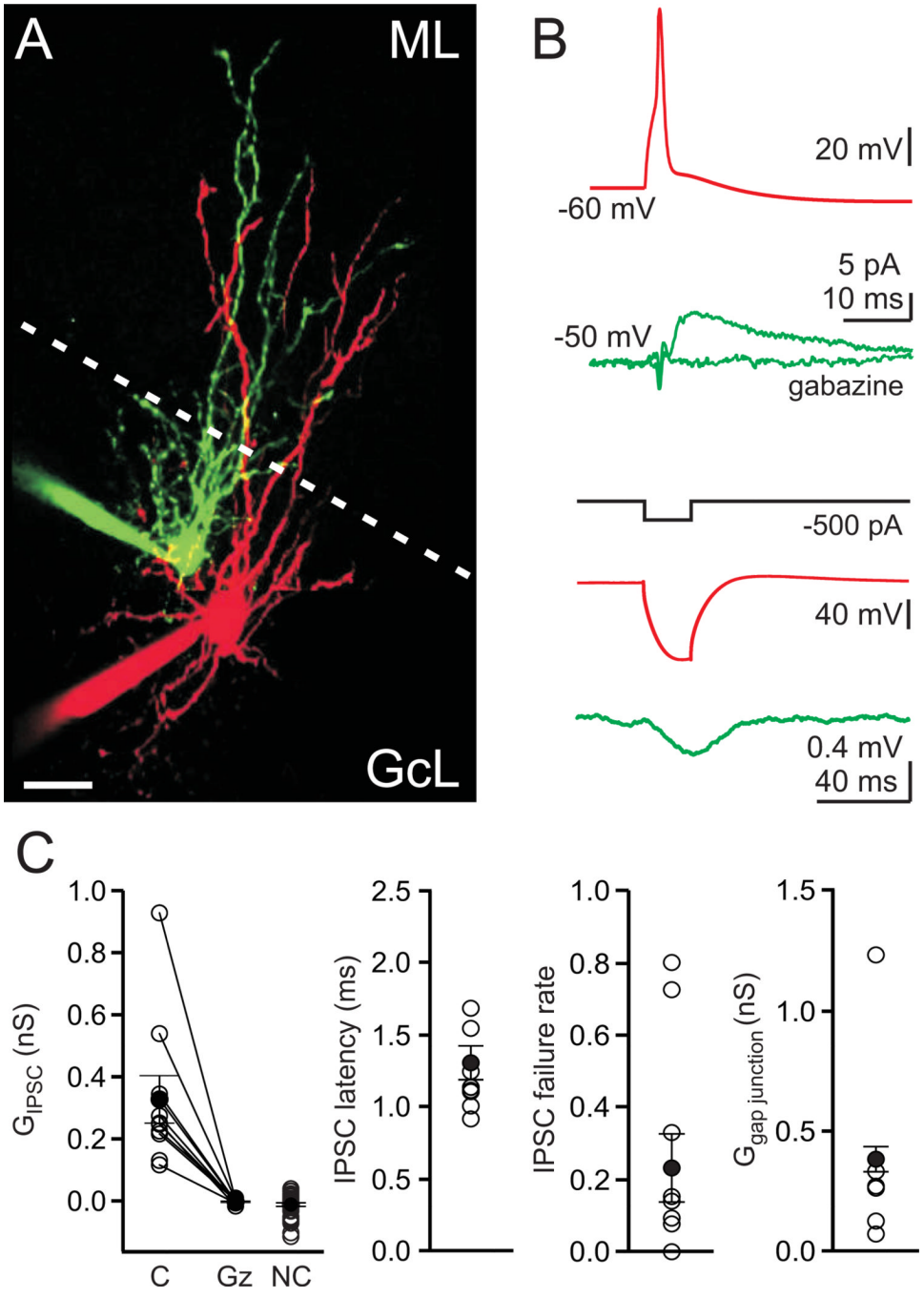

Figure 4. Paired recordings reveal that Golgi cells make GABAergic synapses onto each other

A. A pair of recorded Golgi cells filled with Alexa 488 (green) and Alexa 594 (red), imaged with 2-photon microscopy. Scale bar=20 μm, ML=molecular layer, GcL=granule cell layer, dotted line is the boundary of the molecular layer. **B.** Experiments to test the electrical and chemical connections between neurons, with traces colored to represent the color of filled neurons in A. *top*, Spiking one Golgi cell produced an IPSC in the other Golgi cell. The IPSC is the average of 30 consecutive trials, and it was blocked by gabazine. *bottom*, A current step in one Golgi cell produced a large hyperpolarization in that cell, and a smaller hyperpolarization in the other Golgi cell, indicating that the cells were electrically coupled. **C.** Summary data from paired recordings (50 directions, 1 pair = 2 tested directions, IPSCs

were observed in 10 of 50 directions tested, 3 pairs reciprocally connected). Individual experiments (open circles) and averages (close circles) are shown. *left to right:* Average conductance, IPSC latency, IPSC failure rate and the mean gap junctional conductance. C = connected, Gz = gabazine, NC = not connected.

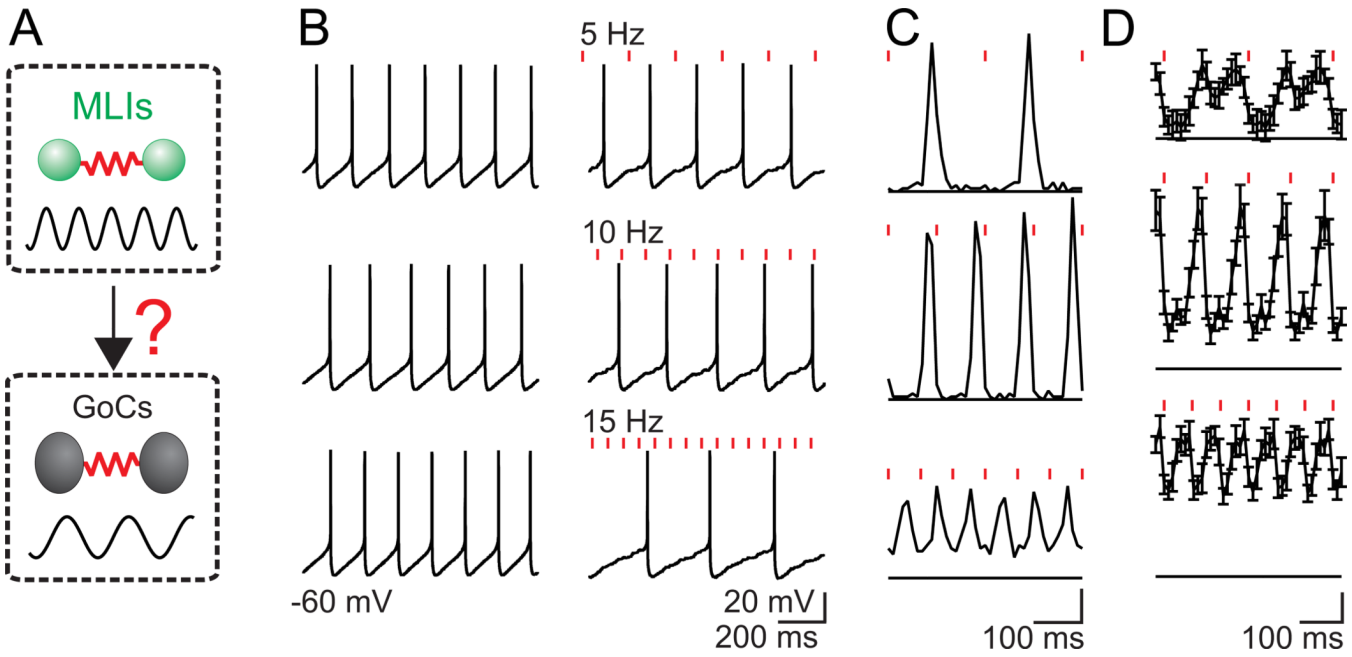

Figure 5. Golgi cell spiking is highly sensitive to small, synchronous inhibitory inputs

A. Schematic showing that MLIs are electrically coupled and can fire synchronously, as is the case for Golgi cells. Dynamic clamp experiments were designed to test the implications of weak cross-network synaptic connectivity from MLIs to Golgi cells (**B–D**). **B.** Golgi cells were allowed to fire spontaneously at 2 to 8 Hz (B, left) and then inhibitory synaptic conductances (IPSGs, 0.5 – 1 nA) with the time course of inhibitory synaptic currents recorded in Golgi cells (E_{IPSG} = −75 mV) were imposed at 5, 10 and 15 Hz (**B**, right) to mimic a weak inhibitory input from the MLI network. **C.** The resulting peristimulus time histograms (PSTH) for the experiment in B shows that inhibition from the MLI network would lead to phase locking of the Golgi cell network. Scale bar (in events/bin/stimulus) top = 0.02 middle = 0.04, bottom = 0.06 **D.** The average PSTH for 14 experiments also show Golgi cell firing phase locked with its inhibitory inputs. Scale bar (in events/bin/stimulus) top = 0.01 middle = 0.02, bottom = 0.03. Bin widths = 10 ms.

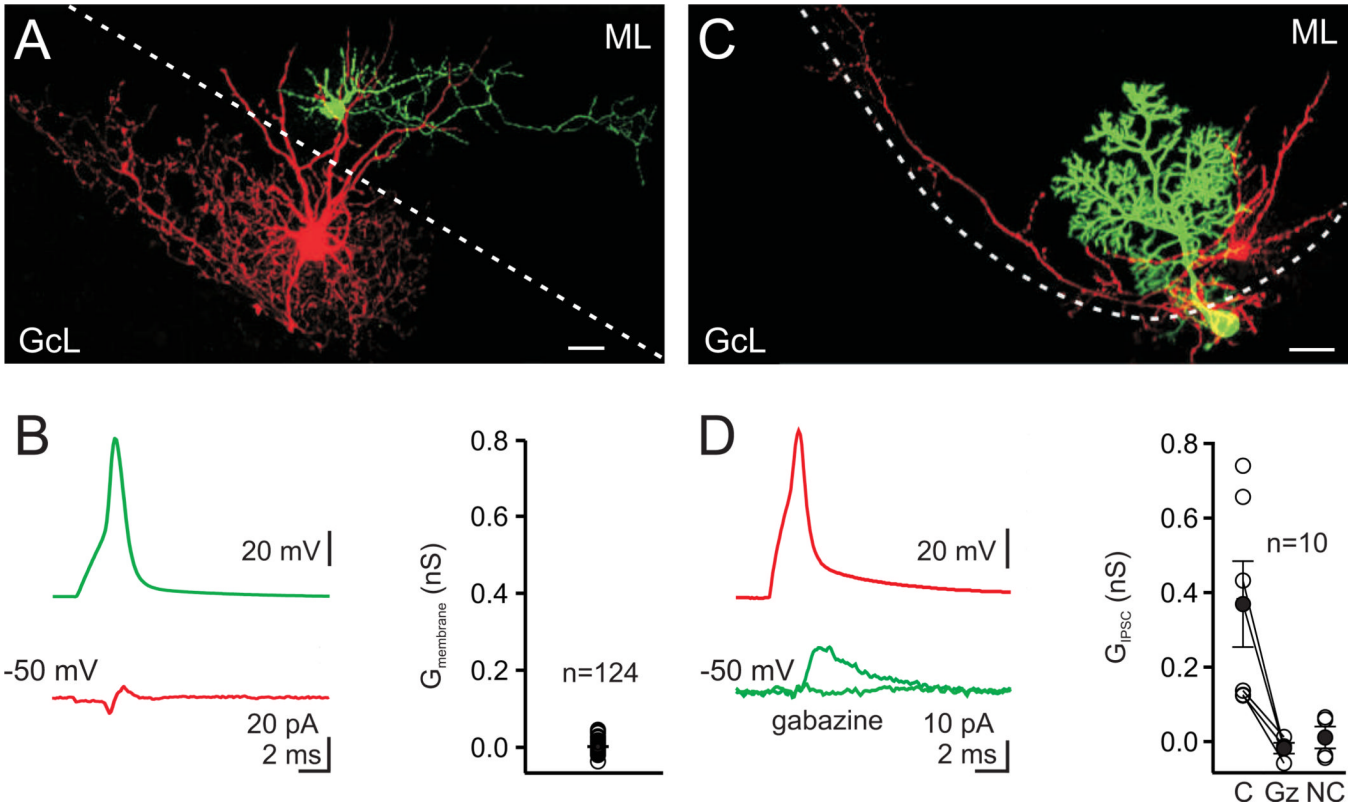

Figure 6. Paired recordings show no connections between molecular layer interneurons and Golgi cells

A. A MLI cell filled with Alexa 488 (green) and a Golgi cell filled with Alexa 594 (red), were imaged with 2-photon microscopy. Scale bar=20 μm, ML=molecular layer, GcL=granule cell layer, dotted line is the boundary of the molecular layer. **B.** *left*, Spiking the MLI (green trace) did not produce an IPSC in the Golgi cell (red trace, average of 70 consecutive trials, inflection is a capacitative electrical artifact). *right*, the average membrane conductance measured from 61 unconnected pairs was 0.001 nS. **C.** Paired recording from a MLI (basket cell, red) and a Purkinje cell (green). **D.** *left*, Spiking the MLI produced an IPSC in the Purkinje cell that was abolished by gabazine (5 μM). *right*, IPSCs were observed In 6 of 10 paired recordings between MLIs and Purkinje cells. C= connected, Gz = gabazine, NC = not connected.

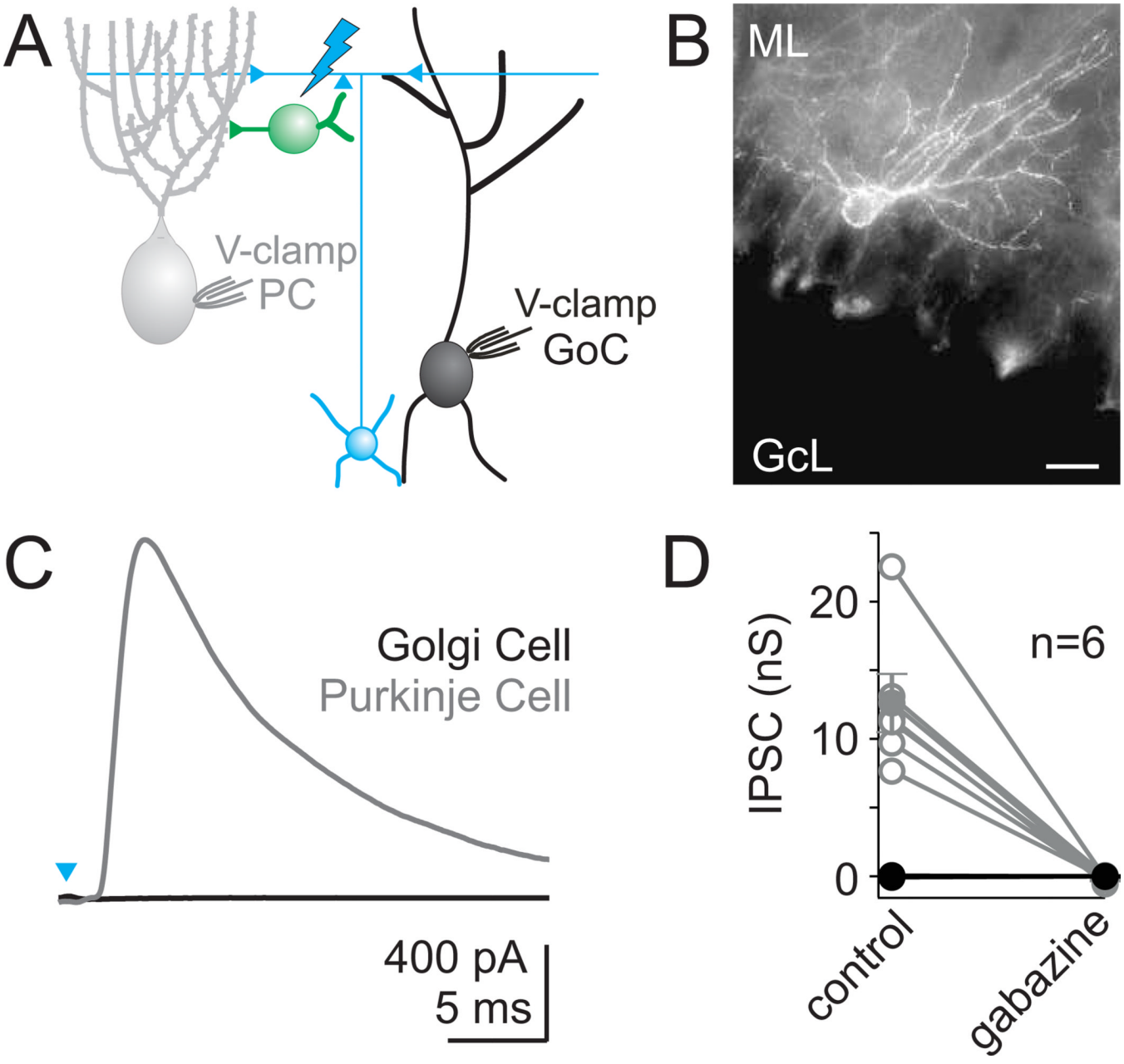

Figure 7. Transgenic mice expressing ChR2 in MLIs demonstrate a lack of fast inhibitory synapses onto Golgi cells

A. Schematic depicting the paired whole-cell recordings of light-activated currents made simultaneously from a Golgi cell and a Purkinje cell in Prv-mhChR2-YFP mice. **B.** A fluorescence image shows intense YFP fluorescence in MLIs. Scale bar = 20 μm **C.** Example of a light-evoked IPSC recorded from a Purkinje cell, with no evoked current in a simultaneously recorded Golgi cell. **D.** Six such experiments are summarized for Purkinje cells (grey) and Golgi cells (black). No currents were evoked in any Golgi cells, and currents in Purkinje cells (mean conductance = 12.6 nS) were completely blocked by the $GABA_A$ receptor antagonist gabazine.

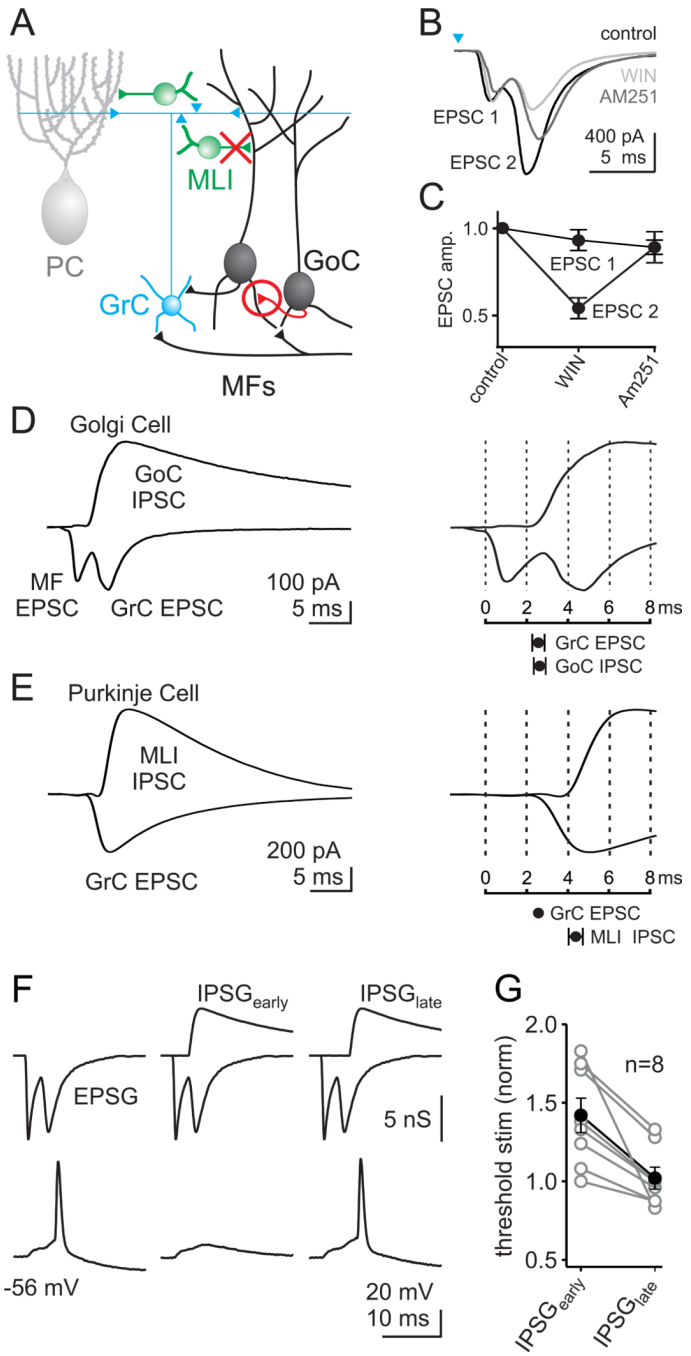

Figure 8. The timing of Golgi cell inhibition matches the timing of granule cell excitation

A. Schematic depicting our revision to the cerebellar circuit diagram. Golgi cells make GABAergic inhibitory synapses onto each other (red circle), and MLIs do not make synapses onto Golgi cells (red X). **B.** Light activation (0.2 ms, 473 nm) evoked an excitatory current onto a Golgi cell with two distinct components (EPSC1 and EPSC2), in control (black). EPSC2 was reduced in the presence of the type 1 cannabinoid receptor (CB1R) agonist WIN (3 μM; light gray) and recovered by the additional application of the CB1R antagonist AM251 (3 μM; dark gray). **C.** The effects of the CB1R agonist and antagonist on EPSC1 and EPSC2 are summarized, and each component is normalized to its initial value in control conditions. **D.** *left*, Example Golgi cell recording where the same light stimulus

produces a dual component EPSC at the IPSC reversal potential, and a disynaptic IPSC at the EPSC reversal potential. *right top*, The same recording on an expanded time scale shows that the onset of EPSC2 (GrC EPSC) closely matches the onset of the Golgi-cell-mediated IPSC. *bottom*, On average, the GrC excitation begins at the same time as Golgi-cell-mediated inhibition (delay = 0.1 ms; n =11). **E.** *left*, A similar experiment as in D is shown, but while recording from a Purkinje cell. Note that the EPSC onto the Purkinje cell only has one component (from the GrCs). *right top*, Same recording on an expanded time scale, with the GrC EPSC set to the timing of the GrC EPSC from D. *bottom*, On average, the GrC excitation precedes the inhibition from MLIs (delay = 1.8 ms; n = 12). **F.** An example of a dynamic clamp experiment that tests the function of Golgi cell inhibition, and the importance of the timing of this inhibition. The timing and amplitudes of synaptic conductances were based on light-activated responses as in **D.** Excitatory inputs consisted of an initial mossy fiber component followed by a granule cell component. In the absence of inhibition, this combined input could evoke action potentials for a threshold level stimulus (**F**, *left*). In this regime, properly timed inhibition robustly suppressed spiking (**F**, *middle*). If the inhibition was delayed, as it would be if it resulted from MLI synapses, the inhibition failed to suppress spiking (**F**, *right*). **G.** Experiments were performed in which the size of the EPSG was varied to determine the threshold for triggering a spike. This was repeated in the presence of properly timed inhibition ($IPSG_{early}$) and late inhibition ($IPSG_{late}$). The effects of inhibition on threshold are summarized by normalizing to the level of threshold stimulus measured in the absence of inhibition. Individual experiments (open circles) and averages (closed circles) are shown.